SF2A 2013
L. Cambrésy, F. Martins, E. Nuss and A. Palacios (eds)

3D SIMULATIONS OF INTERNAL GRAVITY WAVES IN SOLAR-LIKE STARS

L. Alvan[1], A.-S. Brun[1] and S. Mathis[1]

Abstract. We perform numerical simulations of the whole Sun using the 3D anelastic ASH code. In such models, the radiative and convective zones are non-linearly coupled and in the radiative interior a wave-like pattern is observed. For the first time, we are thus able to modelize in 3D the excitation and propagation of IGWs in a solar-like star's radiative zone. We compare the properties of our waves to theoretical predictions and results of oscillation calculations. The good agreement obtained allow us to validate the consistency of our approach and to study the characteristics of IGWs. In the 3D domain, we focus on the excitation of IGWs and on the form of their spectrum where we suspect that both g-modes and propagative waves are present.

Keywords: hydrodynamics, waves, stars: oscillations, methods: numerical

1 Introduction

Internal gravity waves (IGWs) can propagate deeply in radiation zones. For this reason, they are essential to probe stellar interiors (Garcia et al. 2007) and to understand angular momentum transport in stars (Charbonnel & Talon 2005; Mathis et al. 2013). The work presented here follows Alvan et al. (2012) and Mathis et al. (2013). We present results of numerical simulations of a solar-like star where convective and radiative zones are coupled, resulting in the excitation of internal gravity waves. We first present two new developments of the Anelastic Spherical Harmonic (ASH) code and then focus on recent results concerning gravity waves.

2 Recent improvements in the ASH code

In order to study the generation of internal gravity waves by convective motions in solar-like stars, we use the anelastic spherical harmonic (ASH) code (Brun et al. 2004). Our model nonlinearly couples a convective envelope to a stable radiative interior (Brun et al. 2011), assuming a realistic solar stratification from r = 0 up to 0.97R (Brun et al. 2002), by solving the full set of anelastic equations in a rotating spherical shell.

$$\vec{\nabla}.\left(\bar{\rho}\vec{\mathrm{v}}\right) = 0 \tag{2.1}$$

$$\bar{\rho}\left(\frac{\partial\vec{\mathrm{v}}}{\partial t}+\left(\vec{\mathrm{v}}.\vec{\nabla}\right)\vec{\mathrm{v}}\right) = -\vec{\nabla}P+\rho\vec{\mathrm{g}}-2\bar{\rho}\vec{\Omega}_0\times\vec{\mathrm{v}}-\vec{\nabla}.\vec{\mathcal{D}}-\left[\vec{\nabla}\bar{P}-\bar{\rho}\vec{\mathrm{g}}\right] \tag{2.2}$$

$$\begin{aligned}\bar{\rho}\bar{T}\frac{\partial S}{\partial t}+\bar{\rho}\bar{T}\vec{\mathrm{v}}.\vec{\nabla}\left(S+\bar{S}\right) &= \bar{\rho}\epsilon+\vec{\nabla}.\left[\kappa_r\bar{\rho}c_p\vec{\nabla}\left(T+\bar{T}\right)+\kappa\bar{\rho}\bar{T}\vec{\nabla}S+\kappa_0\bar{\rho}\bar{T}\vec{\nabla}\bar{S}\right]\\ &+ 2\bar{\rho}\nu\left[e_{ij}e_{ij}-1/3\left(\vec{\nabla}.\vec{\mathrm{v}}\right)^2\right]\end{aligned} \tag{2.3}$$

We note $\bar{\rho}$, $\bar{P}$, $\bar{T}$ and $\bar{S}$ the reference density, pressure, temperature and specific entropy. Fluctuations about this reference state are denoted by ρ, P, T and S. $\mathrm{v} = (\mathrm{v}_r, \mathrm{v}_\theta, \mathrm{v}_\varphi)$ is the local velocity in spherical coordinates in the frame rotating at constant angular velocity $\vec{\Omega}_0$, $\vec{\mathrm{g}}$ is the gravitational acceleration, c_p is the specific heat per unit mass at constant pressure, κ_r is the radiative diffusivity, $\mathcal{D}$ is the viscous stress tensor and ν, κ and κ_0

[1] Laboratoire AIM Paris-Saclay, CEA/DSM-CNRS-Université Paris Diderot, IRFU/SAp, F-91191 Gif-sur-Yvette Cedex, France

are the effective eddy diffusivities. A volume heating term $\bar{\rho}\epsilon$ is also included in these equations, representing the energy generation by nuclear burning.

Two recent improvements in the code have been taken into account in this work. The first one concerns the anelastic treatment. Brown et al. (2012) have performed a detailed study showing that the anelastic equations written above do not conserve energy and instead conserve a stratification weighted pseudo-energy. As a consequence, these equations obtain incorrect frequencies and radial eigenfunctions for gravity waves. To correct this bias in ASH, we have rewritten the set of equations to implement the Lantz-Braginsky-Roberts equations (e.g., Lantz 1992; Braginsky & Roberts 1995; Lantz & Fan 1999; Jones et al. 2009). This is done by introducing a reduced pressure $\bar{\omega} = P/\bar{\rho}$ instead of the fluctuating pressure P and by converting the buoyancy term to a codensity where only entropy fluctuations S contribute to buoyancy. The resulting momentum equation is

$$\frac{\partial \vec{v}}{\partial t} + \left(\vec{v}.\vec{\nabla}\right)\vec{v} = -\vec{\nabla}\bar{\omega} - \frac{S}{c_p}\vec{g} - 2\bar{\rho}\vec{\Omega}_0 \times \vec{v} - \vec{\nabla}.\vec{\mathcal{D}} \tag{2.4}$$

The effect of this correction is visible when we calculate precisely the frequencies of IGWs as presented in the following part. The second change in the code allows us to treat the singularity at the center of the star. Following Bayliss et al. (2007), we have implemented regularity conditions at $r = 0$. Only $l = 1$ modes can go through the center. The detail of this work will be presented in Alvan et. al (2013) (in prep).

3 Internal gravity waves : excitation

These numerical improvements allow us to study with improved accuracy the spectrum of internal gravity waves excited by the turbulent convection. In fig. 1, we represent the radial velocity $v_r/v_{\rm rms}$ where $v_{\rm rms}$ is the root mean square radial velocity at each radius. It shows two consecutive zoom starting from an equatorial slice ($\theta = 90^o$, all φ).

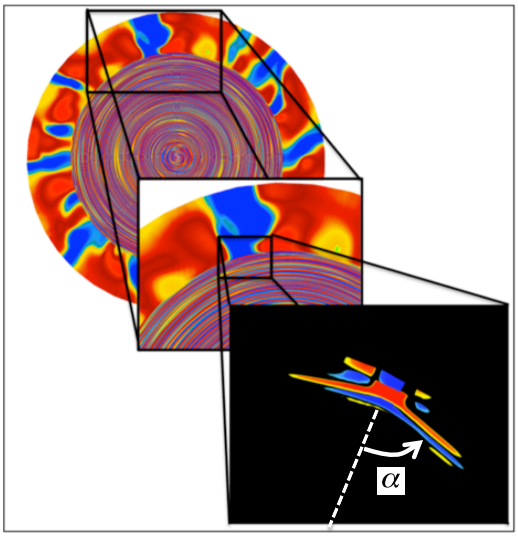

Fig. 1. Gravity waves pattern observed in the radiative (inner) zone and zoom at the base of a downflow (blue) to highlight the St. Andrew's cross. Waves excited by this process have a very low frequency (about 0.01mHz).

In the outer convective zone, we clearly see downward (blue) and upward (red) flows. We observe wavefronts (almost circular spiral) propagating in the radiative zone. To understand the way IGWs are excited we zoom at the base of a downflow. The second zoom shows a classical result of fluid mechanics concerning excitation of IGWs by a localized disturbance in a stably stratified fluid. Waves excited by the pummeling of downward convective flows propagate inside beams, which develop around a St. Andrew's cross in the plane orthogonal to the main direction of the plume. The cross forms an angle α to the vertical given by

$$\alpha = \arccos \frac{\omega}{N}, \tag{3.1}$$

where ω is the frequency of the wave and N the Brunt-Vaisala frequency. In the last zoom, we have distorded the radius in order to highlight the cross. The real value of α is close to 90^o that corresponds to very low frequency waves (about 0.01mHz) and explain the almost circular wavefronts.

4 Internal gravity waves : spectrum

Starting from a temporal sequence of the radial velocity field $V_r(r_0, \theta, \varphi, t)$ at a given depth r_0, we switch from the real space to the spectral space by successively applying a spherical harmonic transform at each time step, which gives $\hat{V}_r(r_0, l, m, t)$, and a temporal Fourier transform on the whole temporal sequence. In Fig. 2, we represent the quantity

$$E(r_0, l, \omega) = \sum_m |\tilde{V}_r(r_0, l, m, \omega)|^2 \qquad (4.1)$$

as a function of frequency ω and order l for three given depths. The spectrum obtained is extremely rich and close to the one predicted by the linear theory.

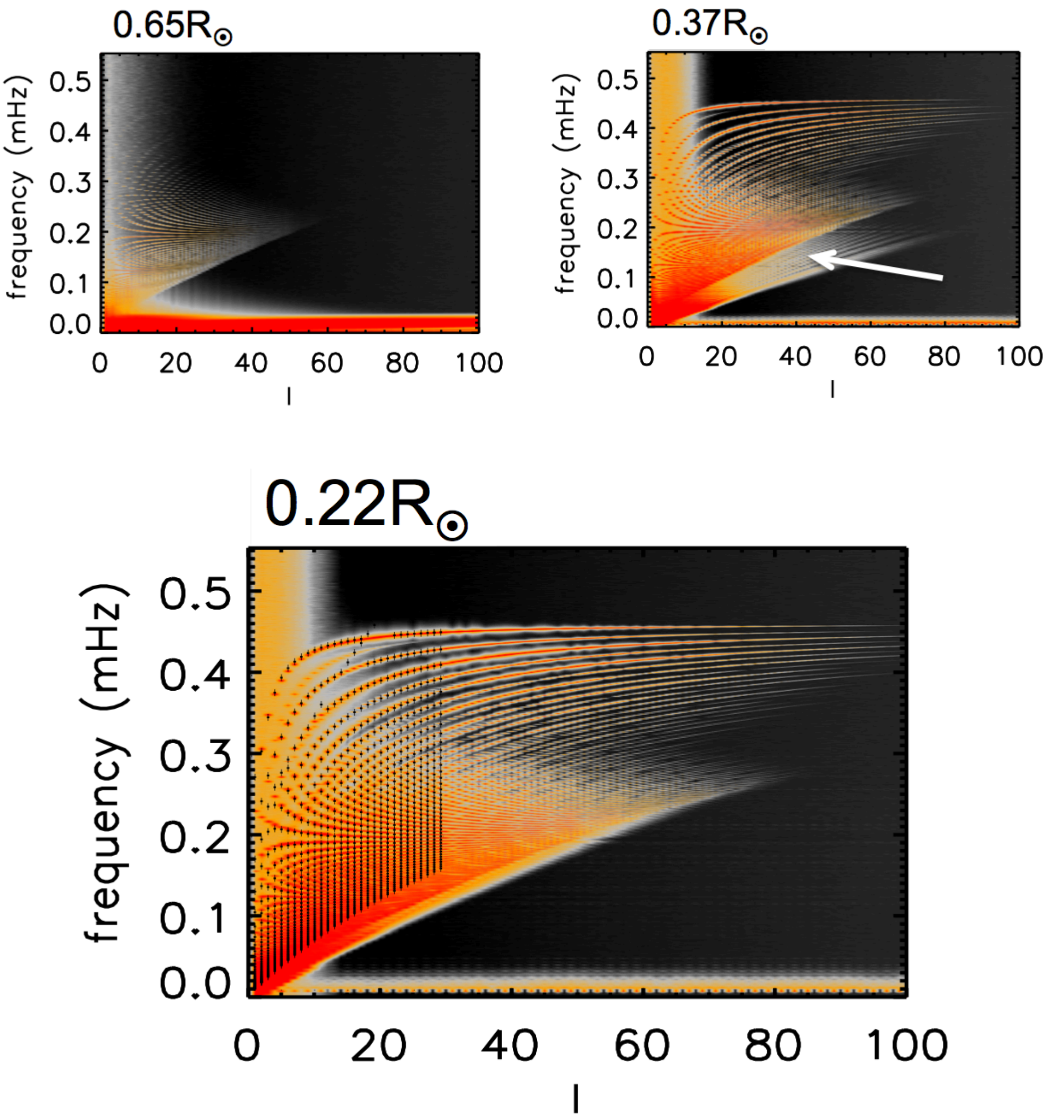

Fig. 2. Spectrum of gravity waves calculated at three different depths in the radiative zone. Black crosses in the panel at r=0.22 $R_\odot$ represent the frequencies obtained by the ADIPLS oscillation code.

In the bigger panel of Fig. 2, we have superimposed the frequencies obtained by the ADIPLS code* to show the good agreement obtained (black crosses). At high frequencies, ridges are formed by modes with the same radial order n (number of zeros in the radial direction in the eigenfunctions). They tend to an asymptote corresponding to the maximum value of the Brunt-Vaisala frequency N. We note that the spectrum's global aspect is different depending on the depth. We do not show the convective zone since no modes are visible. Indeed, IGWs are evanescent in regions where the entropy gradient is negative. At $0.65R_{\odot}$, where $R_{\odot}$ is the solar radius, only the low frequency part of the spectrum is observed and a big bump of energy is visible (in red) at very low frequency. We suspect it to correspond to very low frequency waves excited by plumes as explained in the previous section. In the second panel corresponding to $0.37R_{\odot}$, the spectrum is more complete but we see a region looking different of the rest at low frequency. The energy in this region does not form peaks regularly spaced in period, such as g-modes should do. Consequently, we interpret this region as propagating gravity waves that do not form g-modes. The fact that this zone reduces and disappears when we move down into depth reinforces this hypothesis since it corresponds to the action of the radiative damping on these waves.

5 Conclusions

We have shown that a detailed analysis of IGWs in 3D non-linear dynamical simulations is possible. For the first time, we are able to model the behaviour of both propagative and standing waves in a realistic 3D cavity. The results presented here do not take into account the rotation of the model since we have added up all the asimuthal number m. But the contribution of 3D simulations is also important for studying the effect of the rotation on gravity waves and for measuring rotational splitting. Moreover, excitation rates could be applied as an input for dynamical stellar evolution codes such as STAREVOL.

The authors warmly thanks the SF2A organizing committee and the four editors of the proceedings. We also acknowledge financial support by ERC STARS2 207430 project, by CNES - GOLF and FP7-IRSES, and access to supercomputers through GENCI project 1623.

References

Alvan, L., Brun, A. S., & Mathis, S. 2012, in SF2A-2012: Proceedings of the Annual meeting of the French Society of Astronomy and Astrophysics. Eds.: S. Boissier, 289–293

Bayliss, R. A., Forest, C. B., Nornberg, M. D., Spence, E. J., & Terry, P. W. 2007, Physical Review E, 75, 26303

Brown, B. P., Vasil, G. M., & Zweibel, E. G. 2012, astro-ph

Brun, A. S., Antia, H. M., Chitre, S. M., & Zahn, J.-P. 2002, Astronomy and Astrophysics, 391, 725

Brun, A. S., Miesch, M. S., & Toomre, J. 2004, ApJ, 614, 1073

Brun, A. S., Miesch, M. S., & Toomre, J. 2011, ApJ, 742, 79

Charbonnel, C. & Talon, S. 2005, Science, 309, 2189

Garcia, R. A., Turck-Chièze, S., Jiménez-Reyes, S. J., et al. 2007, Science, 316, 1591

Mathis, S., Decressin, T., Eggenberger, P., & Charbonnel, C. 2013, Astronomy and Astrophysics, 558, 11

*Christensen-Dalsgaard, J. 2011, *ADIPLS: Aarhus Adiabatic Oscillation Package (ADIPACK)*